Indian Journal of Chemistry
Vol. 65, January 2026, pp. 24-31
DOI: 10.56042/ijc.v65i1.23315

# Weak intermolecular interactions modulate supramolecular synthon: A combined X-ray powder diffraction and Hirshfeld surface analysis

Suniti Pradhan[a], Susanta Mandal[b], Sayantari Ghosh[b], Abir Bhattacharya[c] & Dipak K Hazra*[a]

[a] Department of Physics and Coastal Environmental Studies Research Centre, Egra S. S. B. College, Purba Medinipur 721 429, West Bengal, India

[b] Department of Physics, National Institute of Technology Durgapur, Durgapur 713 209, West Bengal, India

[c] Department of Physics, The Bhawanipur Education Society College, Kolkata 700 020, West Bengal, India

E-mail: dipakkhazra@gmail.com

*Received 1 September 2025; accepted (revised) 5 January 2026*

Crystal structure of 4-oxo-4*H*-chromene-3-carbaldehyde (**I**) has been investigated from X-ray powder diffraction data along with Hirshfeld surface analysis and associated 2D fingerprint plot. A comparison of intermolecular interaction of related compound shows the contribution of weak intermolecular interactions tuned the supramolecular assembly forming $C_1^1(5)$, $C_1^1(3)$ polymeric chain and $R_1^1(8)$, $R_4^4(20)$ rings generating two-dimensional honeycomb framework. Hirshfeld surface analysis of (**I**) and a few related chloro/bromo/iodo derivatives obtained from CSD also shows that moderately weak inter molecular interactions play a significant role in crystal packing arrangement. Additionally, interpretation of Full Interaction Map (FIM) also supports the observed packing arrangement of the title compound.

**Keywords:** *Ab-initio* structure determination, Weak intermolecular interaction, Supramolecular assembly, Hirshfeld surface analysis, HOMO-LUMO gap, Full Interaction Map

Heterocyclic compounds have attracted significant attention for their structural versatility and wide range of applications in medical and biological sciences[1-8]. The research interest of heterocyclic compound is growing rapidly due to their functional variation[2-4]. Heterocyclic compounds are ring structures that contain at least one hetero atom present in the backbone[9,10]. The fusion of heterocyclic ring with oxygen atom with dominant electron density affects physical, chemical and biological properties of the heterocyclic composites[11]. More specifically oxygen atom containing heterocyclic are made of more attention in organic chemistry for medicinal use as drugs (cumarin and oxaltole), Solvent (tetrahydrofuran)[11,12]. Chromene are heterocyclic compounds fused with benzene and pyran moiety is found in a variety of natural and synthetic compound with several biological activities[13-15]. The compounds with 4H-chromene ring having double bond to a hetero oxygen atom are the important scaffold of pharmacological industry with wide range of applications such as anti-bacterial[16,17], anti-viral[18], anti-malaria[19], anti-cancer[20-22], *etc*. In recent year, 3-formyl chromone derivatives have gained a notable attention as a highly reactive compounds due to the presence of keto group at C3 carbon atom and a conjugated carbonyl group at C2 possess highly polarised π-bond in C1-C2[23,24].

Non covalent interactions in particular hydrogen bond D-H... A (D=donor, A=acceptor) act as a important role in supramolecular chemistry and crystal engineering[25,26]. Supra molecular aggregation by electronegative N and O atom is often form strong hydrogen bonds with estimated interaction energy 15 -50 kJ/ mole and D-H…A ≥ 160º. The hydrogen bonds lead to the supramolecular extended assembly built from relatively small synthon with aromatic motifs. In addition to this strong hydrogen bond the weak interaction C-H…O/N, C-H…π, and π-π stacking moderate to low electronegativity can impact significantly to form supramolecular motifs in organic compounds[27]. Although each interaction is relatively weak and no precise geometry, but their combine effect, can be modulate significantly as strong interaction[28,29]. In this context, we report here the contribution of different C-H…O intermolecular interactions to build supramolecular assembly in chromene derivatives. An investigation of close intermolecular interaction in (**I**) and few related chromene derivative with Z= 2 *via* Harshfield surface

analysis is also presented along with quantum mechanical calculation to investigate the molecular geometry and their properties.

Structure determination from single-crystal X-ray diffraction analysis is now the preferred choice. Inherent limitation to grow single crystal of perfect size and quality that make them unsuitable for structural characterization. Since many valuable compounds are only available in microcrystalline powders, so X-ray powder diffraction method is only reliable alternative option for crystal structure determination. To assess the reliability of crystal structure determination of (**I**) from PXRD with earlier reported structure (code: AMITEW)[30] from single crystal structure analysis was redetermined and compared with different molecular properties.

## Experimental Section

### Materials and X-ray data collection

The compound 4-oxo-4H-chromene-3-carbaldehyde was purchased from Sigma Aldrich and utilized directly without additional purification. X-ray powder diffraction data of compound (**I**) was collected at 293(2)K using a Bruker D8 Advance powder diffractometer with CuKα radiation (λ = 1.5418 Å) in Bragg–Brentano geometry.

### Indexing and structure analysis

The indexing of X-ray powder diffraction pattern of the compound (**I**) was carried out using the NTREOR program[31] with full pattern decomposition by EXPO2004[32], employing the Le Bail algorithm[33], and utilizing a split-type pseudo-Voigt peak profile function[34]. Statistical analysis of the powder patterns, conducted *via* the FINDSPACE module in EXPO2004, identified $P_{21}$ as the most likely space group for this compound, which was subsequently used for the structure solution. Structure solution of this compound was determined through global optimization of structural models in direct-space, based on Monte-Carlo search using the simulated annealing technique (in parallel tempering mode), as implemented in FOX[35]. The input of the initial geometry was determined by MOPAC 9.0[36]. A chemically sensible packing models with no reasonable discrepancies between the observed and calculated powder patterns were selected as the starting models for the Rietveld refinement[37], which was performed using the GSAS program[38] with the EXPGUI interface[39]. The background was modelled using a shifted Chebyshev function of the first kind, with 15 points uniformly distributed over the full 2θ range for this compound. Initial refinements were focused on the lattice constants, background coefficients, and profile parameters, and subsequent refinement of the positional co-ordinate of the non-hydrogen atom. Soft restraints were applied to maintain reasonable bond distances and angles, as well as planarity of the molecule without aldehyde oxygen (O13) atom to keep free to move. A constant isotropic displacement parameter of 0.0126 Å² was applied for all non-hydrogen atoms. H atoms were positioned in calculated locations with a common $U_{iso}$ value of 0.025 Å². In the final refinement stages, a preferred orientation (18) correction was applied through the generalized spherical harmonic model.

### Hirshfeld surface analysis

Hirshfeld surfaces[40] and corresponding 2D fingerprint plots[41] were generated using Crystal Explorer[42], which analyse the structure as a crystallographic CIF format. Hydrogen atom bond lengths were set to standard neutron values (C-H = 1.083 Å and N-H = 1.009 Å). The $d_{norm}$ surface is visualized using a red–white–blue colour scale, where bright red regions indicate shorter interactions, white areas signify contacts near van der Waals distances, and blue regions show an absence of close contacts.

### DFT Calculations

Quantum mechanical calculations of the isolated molecule were performed *via* DMol3[43] code incorporated in BIOVIA DISCOVERY STUDIO using the functional B3LYP[44] to optimize the geometry of the molecule with energy minimization. The source of initial atomic positions was picked from final refinement cycle. The quality of the calculation was kept in fine mode and during the calculations, apart from the binding energy, the HOMO and LUMO energy is also being calculated along with their formation region inside the molecule. Energy optimization was performed without imposing any constraints on the structural moiety allowing the molecule to adopt the most stable confirmation freely.

## Results and Discussion

### Crystal and molecular Structure

The crystal structure of (**I**) has been determined using X-ray powder diffraction data. The final Rietveld refinement plot shows a very good matching between the experimental and calculated powder patterns (Fig. 1), with low residual values for $R_p$, $R_{wp}$,

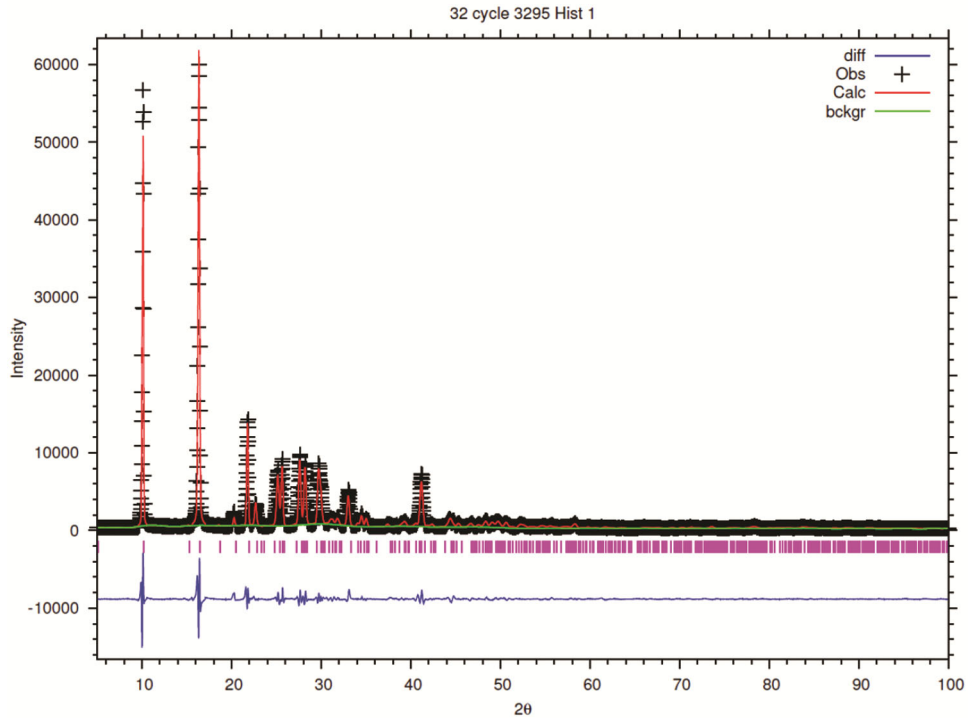


Fig. 1 — Final Rietveld plot for $C_{10}H_6O_3$. Black cross: observed pattern, Red curve: calculated pattern, Blue curve: difference curve.

Table 1 — Crystal data and Rietveld refinement parameters of (I) 4-oxo-4*H*-chromene-3-carbaldehyde

| | |
|---|---|
| Chemical formula | $C_{10}H_6O_3$ |
| Formula Weight | 174.15 |
| Temperature | 293(2)K |
| Crystal System | Monoclinic |
| Wavelength(Å) | 1.5418 |
| Space Group | $P_{21}$ |
| a(Å) | 17.372(1) |
| b(Å) | 5.656(1) |
| c(Å) | 3.889(2) |
| α(º) | 90.0 |
| β(º) | 91.646(6) |
| ϒ(º) | 90.0 |
| Volume(Å$^3$) | 381.954(24) |
| Z | 2 |
| Density(calculated) g cm$^{-3}$ | 1.5142 |
| 2Θ interval(º) | 5-100 |
| Step Size(º) | 0.02 |
| Counting time/step(s) | 4 |
| No. of background points refined | 36 |
| $R_p$ | 0.09 |
| $R_{wp}$ | 0.1211 |
| $R_F^2$ | 0.7788 |
| $\chi^2$ | 16.28 |

and $\chi^2$ (Table 1) having higher space group symmetry $P_{21}$ (50191 hits) is more compared with the structure determination having space group $P_c$ (in AMITEW) (1923 hits) is one of the most frequently encountered space group both organic and inorganic materials in

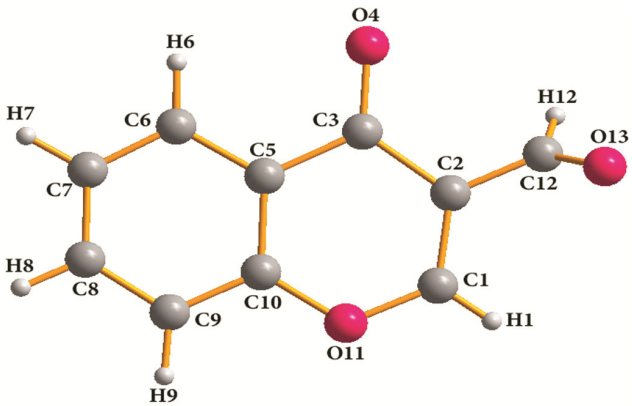


Fig. 2 — Molecular structure of $C_{10}H_6O_3$ with atom labelling scheme.

crystallography. In PXRD, three-dimensional (3D) diffraction data compressed into one dimension (1D) leads to higher space group symmetry constitute same chemical information considering all possible crystal orientation on average. As a result, powder diffraction pattern exhibits significant overlapping of peaks makes it more challenging in *ab-initio* structure determination from PXRD[45]. All the subsequent analysis and discussions of compound (**I**) have been reported here based on the X-ray powder diffraction analysis.

The molecular view of title compound (**I**) with atom numbering scheme is shown in Fig. 2. A summary

of the crystallographic data along with related refinement parameters are given in (Table 1). In the title compound (**I**), non-hydrogen atoms excluding aldehyde O atom (O13) are essentially planer with r.m.s deviation 0.0104Å with the most significant deviation from the least square plane 0.0417Å being for the chromene-ring carbon atom (C2). However, the aldehyde O atom (O13) is twisted from the least square plane by the torsion angle C1-C2-C12-O13 = –51.36° and C3-C2-C12-O13 = 121.97°. The observed bond length and angles (Table 2) agrees well with the analogues structure reported in the literature[46,47].

The C-H…O Interaction considered as weak hydrogen bonds based on the 3.0 < D…A < 3.5 Å, 2.2 < H…A < 2.8 Å, and 120° < D-H…A < 180° criteria[48]. As C-H…O interaction individually weaker but their combined effect act as a strong hydrogen bond effects in supramolecular assembly [28,29]. In (I), molecules are connected by different C-H…O hydrogen bonds (Table 3). The chromene C atom (C1) in the the molecule at (x,y,z) acts as a hydrogen bond donor through H1 to the chromene O atom (O4) in the molecule at (x,y+1,z+1) generating an infinite $C_1^1(5)$ chain denoted by AAAA… (Fig. 3) along [011] direction. Similar hydrogen bond connected by the benzene C atom (C6) acts as a donor to the chromene O atom (O11) (x,y-1,z-1**)** generating an infinite chain $C_1^1(5)$ denoted by BBBB… propagating along [011] direction (Fig. 3). In addition to these weak interaction another hydrogen bond produced by aldehyde carbon atom (C12) in the molecule (x,y,z) further connected to aldehyde O atom(O13) at (x,y,z-1) generating another possible hydrogen bond $C_1^1(3)$ chain along CCCC… (Fig. 4) [001] direction. The combination of AAAA…. and BBBB…. chains producing $R_1^1(8)$ ring (Fig. 3). Similar $R_4^4(20)$ synthon[49]

Table 2 — Selected bond lengths (Å) and angles (°) for $C_{10}H_6O_3$ (I)

| | | |
|---|---|---|
| Bond lengths (Å) | | |
| C1-C2 | | 1.387(10) |
| C1-O11 | | 1.355(9) |
| C2-C3 | | 1.472(9) |
| C2-C12 | | 1.353(9) |
| C3-O4 | | 1.278(10) |
| C3-C5 | | 1.465(9) |
| C5-C10 | | 1.422(9) |
| C10-O11 | | 1.348(10) |
| C12-O13 | | 1.157(10) |
| Bond angles (°) | | |
| C2-C1-O11 | | 122.5(6) |
| C1-C2-C3 | | 120.1(5) |
| C1-C2-C12 | | 122.7(6) |
| C3-C2-C12 | | 116.8(6) |
| C2-C3-O4 | | 124.1(6) |
| C2-C3-C5 | | 115.2(5) |
| O4-C3-C5 | | 120.6(6) |
| C3-C5-C10 | | 119.4(5) |
| C5-C10-O11 | | 121.8(5) |
| C1-O11-C10 | | 120.8(6) |
| C2-C12-O13 | | 120.0(5) |
| C2-C12-H12 | | 118.9(6) |
| O13-C12-H12 | | 121.1(6) |
| Torsion angles (°) | | |
| C1-C2-C12-O13 | –51.36° | |
| C3-C2-C12-O13 | 121.97° | |

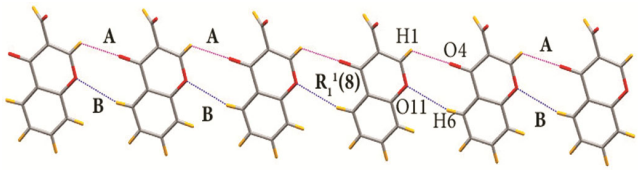


Fig. 3 — A view of $R_1^1(8)$ ring running along the [011] direction in $C_{10}H_6O_3$.

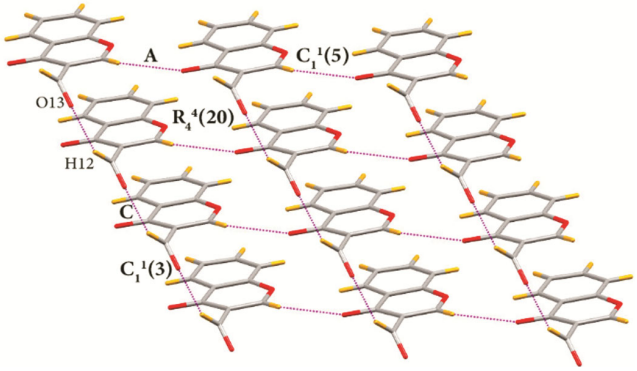


Fig. 4 — A view of $R_4^4(20)$ synthon generated by $C_1^1(5)$ and $C_1^1(3)$ chain in the structure of $C_{10}H_6O_3$.

Table 3 — Hydrogen bonding geometry (Å, °) for $C_{10}H_6O_3$

| D-H….A | d(D-H) | d(H….A) | d(D……A) | <(DHA) | [Symmetry transform] |
|---|---|---|---|---|---|
| C12-H12….O13 | 0.941 | 2.095 | 2.818 | 132 | [X,Y,Z-1] |
| C1-H1….O4 | 0.883 | 2.611 | 3.240 | 128 | [ X,Y+1,Z+1] |
| C6-H6….O11 | 0.943 | 2.834 | 3.742 | 161 | [X,Y-1,Z-1] |
| Cg….Cg | – | – | 3.888 | – | [X,Y,-1+Z] |

Cg is the centroid of 6-membered ring (C5-C10)

is generated by $C_1^1(5)$ and $C_1^1(3)$ chain (Fig. 4) built a two-dimensional (Fig. 5) fused supramolecular honeycomb network. Using Aromatic Analyzer tool of Mercury within CCDC, an analysis of the geometries of intermolecular interaction between the aromatic rings shows a strong π-π interaction with centroid-centroid distance is 3.89Å.

## Hirshfeld surface and 2D fingerprint plot

Hirshfeld surfaces[50] analyse the packing patterns and interpretation of non-covalent interactions maintaining a holistic approach to the entire molecule. These surfaces are generated by dividing the crystal space into regions where the electron density is derived from the sum of the spherical atoms of the molecule larger than corresponding sum across the crystal[51]. 2D fingerprint plots[41] provide a quantitative representation of the nature and types of intermolecular interactions. This type of analysis is particularly useful for identifying and quantify both the common features and subtle variations in non-covalent interactions among different polymorphic form and correlated compounds[52,53].

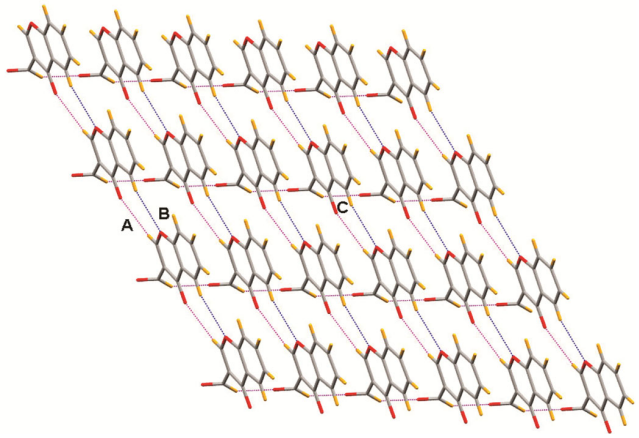


Fig. 5 — Two-dimensional honey-comb structure of $C_{10}H_6O_3$ in supramolecular framework.

The Hirshfeld surface of the compound (**I**) is depicted in Fig. 6A, with the surfaces plotted over a $d_{norm}$ range of –0.5 to 1.0 Å. A colour gradient was used, where red indicates shorter $d_{norm}$ values, and blue represents longer $d_{norm}$ values. The most dominant interactions in the molecule can be visualise in the Hirshfeld surface as red areas marked as '**a**' due to O13-H12 hydrogen bond and relatively weak interaction generated by C1-H1…O4 are shown in the Hirshfeld surface are marked as '**b**' in the title compound (Fig. 6A).

The associated 2D fingerprint plot (Fig. 6B) demonstrates characteristic spike in the region $1.9<d_e+d_i<2.7$ (labelled as '**c**' and '**d**') resulting from different types of C-H…O interaction. The upper spike '**c**' denotes the donor spike (aldehyde, chromene and phenyl CH group H atom interacting with aldehyde and chromene oxygen O13, O4, O11 atom) and lower spike '**d**' represents the acceptor spike (aldehyde and chromene oxygen O13, O4, O11 atom) interacting with aldehyde, chromene and phenyl CH group H atom) demonstrate the characteristic weak C-H…O interaction. It is also observed that the contribution of H-O interaction is about 27.4% of the total surface area. Further the wings (marked as '**e**' and '**f**') in the $(d_i,d_e)$ regions of (1.2Å, 1.8Å) and (1.8Å, 1.2Å) are assigned to the C-H covalent interaction. The central spike (marked as '**g**') stretching upto $(d_i,d_e)$ region of (1.021Å, 1.036Å) in Fig. 6B reflects a high % of H-H contacts covered 32.9% of the total Hirshfeld surface area.

The relevant contributions of various intermolecular interactions to the Hirshfeld surface were generated for compound (**I**), AMITEW and for few related

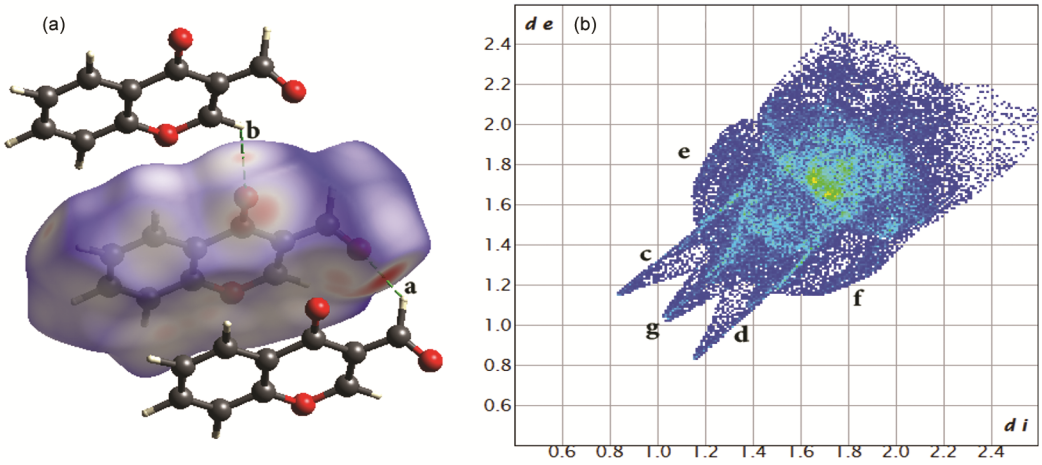


Fig. 6 — (a). Hirshfeld surface and (b). 2D fingerprint plot of title compound (I).

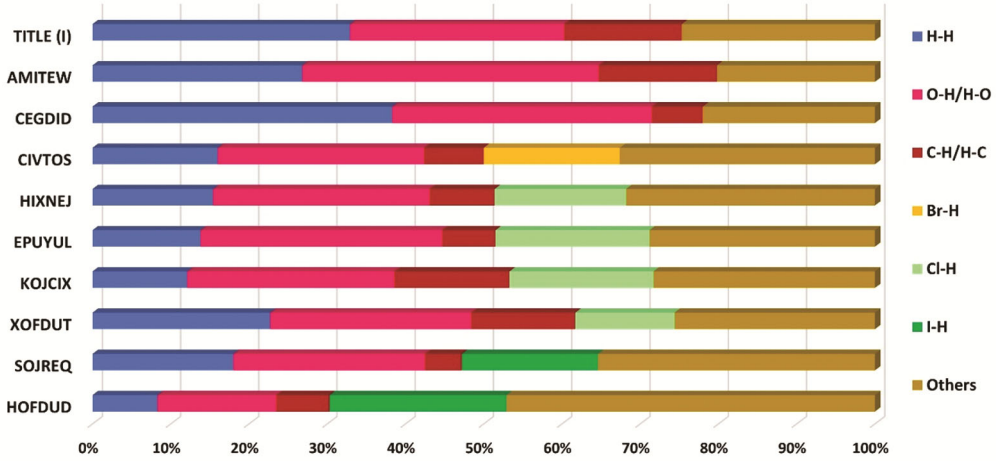


Fig. 7 — The relative contributions of different intermolecular contacts to the Hirshfeld surface area in (I) and few related compounds retrieved from the CSD.

compounds (Z=2) which were similar structure of (I) obtained from CSD are given in (Fig. 7).

It is observed that the total relative contribution of non-covalent interaction H-H, H-O/O-H and C-H/H-C interaction are 75.3% for structure (I) obtained from PXRD and 79.8% for AMITEW agrees well in the of Hirshfeld surface area (Fig. 7). Due to different type of substituents in the phenyl ring, it provides valuable understanding of the role of intermolecular contacts. The similar type of contribution for related structure are about CEGDID[54]] (78%), CIVTOS[55] (49%), HIXNEJ[56] (51%), EPUYUL[57] (51%), KOJCIX[58] (54%), XOFDUT[59] (62%), SOJREQ[60] (48%), HOFDUD[61] (30%). In this context we also study the nature and propensity of the halogen atom in the week intermolecular interaction which plays crucial role for crystal engineering[62,63]. For this purpose, we choose the similar structure related to (I) with different halogen substituents in the moiety. It is observed that the halogen bond C-H...X (X= Cl/Br/I) exploring a significant role in the crystal packing. This is reflected in the relative contribution for the halogen atom (here Cl,Br,I) is about 16.8%[HIXNEJ], 19.7%[EPUYUL], 18.4%[KOJCIX], 12.7%[XOFDUT], 17.4%[CIVTOS], 17.4%[SOJREQ] and 22.6%[HOFDUD] respectively, in addition to the relatively strong H-bond of the entire Hirshfeld surface area. The influence of the various interactions in the Hirshfeld surface area (Fig. 7) arises from changes in the properties of C-H/C-X (X= Cl/Br/I) bond due to high polar nature of the latter[64,65].

## Full Interaction Map

The Full Interaction Map (FIM) incorporated in the CSD (version, 5.46 Nov,2024) creates three-dimensional

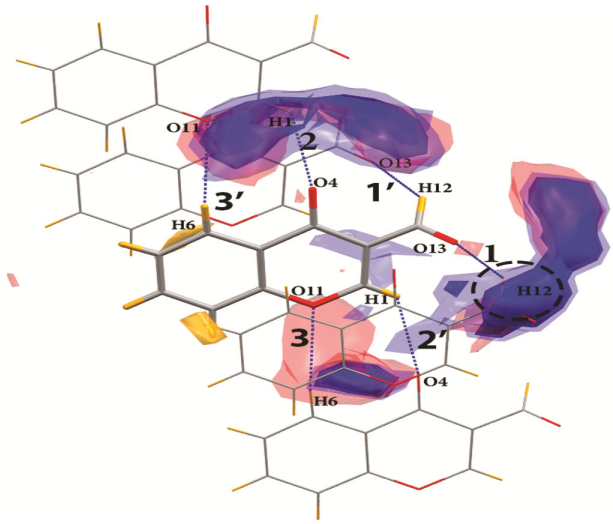


Fig. 8 — Analysis of Full Interaction Maps of title compound $C_{10}H_6O_3$.

visualization of the probabilities of different types of intermolecular interactions within a molecule. Fig. 8 illustrates the full interaction maps for compound (I) that exhibit preferred hydrogen bonding interactions and provide a platform for crystal morphology analysis[66,67]. The blue regions of the interaction map highlight hydrogen bond donor, red regions indicate likely position of hydrogen bond acceptor and brown region represent hydrophobic preferences[68]. The interaction maps are visualised using standard contour levels of 2,4,6, with increasing opacity. In this structure, FIM reveals six distinct hotspots along with some additional diffuse interaction region. Among these six interactions, three high probability hydrogen bond donor regions are identified (blue regions: interaction 1,2,3 i,e. O13...H12, O4...H1, O11...H6) and relatively less defined hydrogen

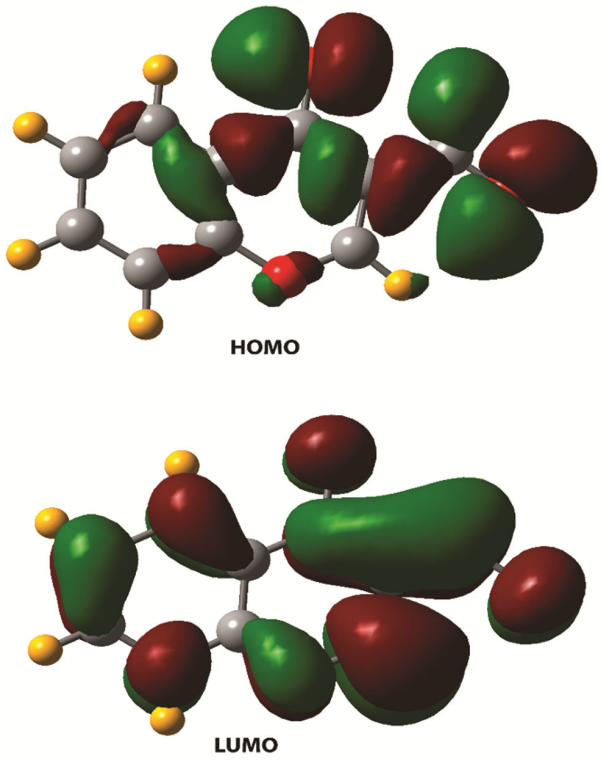


Fig. 9 — HOMO and LUMO population of (**I**).

bond acceptor regions are found (red regions: interaction 1',2',3' *i.e.*, H12…O13, H1..O4, H6...O11). In FIM (marked as black circle) shows the robust donor region centered on the O13 atom of the aldehyde group which is most predictable hydrogen bond acceptor. The existence of weak acceptor peak indicates moderate propensity of the H…O. Additionally small brown region predicts higher probability of aromatic interaction between the two phenyl rings *i.e.*, π-π interactions. Most expected position of the hydrogen bond acceptor and donor map correlate well with the packing arrangement of the title compound governed by weak intermolecular interaction.

## Electronic structure

The total binding energy of the molecule -42.25 Ha in quantum mechanical calculation of (**I**). The molecular orbital energy calculation at the B3LYP level show $E_{HOMO}$ (highest occupied molecular orbital) and $E_{LUMO}$ (lowest unoccupied molecular orbital) values of -0.2576 Ha and -0.0843 Ha respectively. The HOMO–LUMO energy separation indicates kinetic stability of molecule[69,70]. The magnitude of the HOMO–LUMO energy gap is 4.715ev, implies high kinetic stability, which indicates lower reactivity of the molecule. The HOMO and LUMO population are given in Fig. 9.

## Conclusions

The structure determination of (**I**) reveals an interplay of weak intermolecular interactions along with π-π stacking, which together contribute to the formation of a two-dimensional honeycomb framework. A comparison of close intermolecular interactions and several related compounds (retrieved from CSD) using Hirshfeld surface analysis highlights the critical influence of these intermolecular interactions in crystal engineering. In the quantum mechanical calculation, the HOMO-LUMO gap in (**I**) (4.715ev) indicates the higher stability and lower reactivity pattern of the compound.

## Acknowledgement

Financial support from the University Grants Commission, New Delhi, through the DRS (SAP-II) program for purchasing the X-ray powder diffractometer in the Department of Physics, Jadavpur University, is gratefully acknowledged.

## Supplementary Information

Crystallographic data for the structure 4-oxo-4H-chromene-3-carbaldehyde (**$C_{10}H_6O_3$**) reported in this article has been deposited with the Cambridge Crystallographic Data Centre as CCDC Deposition Number 2331190 and. Copy of the data can be obtained free of charge on application to CCDC, 12 Union Road, Cambridge CB2 1EZ, UK (fax: +44 1223 336033; email: (deposit@ccdc.cam.ac.uk).

## Declaration of funding source

This research did not receive any specific grant from funding agencies in the public, commercial, or not-for -profit sectors.

## References

1 Kabir E & Uzzaman M, *Results Chem*, 4 (2022) 100606.
2 Mahmood R M U & Aljamali N M, *Eur J Mol Clin Med*, 7 (2020) 2020.
3 Ogawa Y, Tokunaga E, Kobayashi O, Hirai K & Shibata N, *I Science*, 23 (2020) 101467.
4 Pozharskii A F, Soldatenkov A T & Katritzky A R, *Heterocycles in Life and Society*, (A John Wiley & Sons, Ltd.) 2011.
5 Al-Mulla A, *Der Pharm Chem*, 9 (2017) 141.
6 Kumar P B R, Subramaniyan S, Yamini K & Suthakaran R, *Ras J Chem*, 4 (2011) 400.
7 Shaikh A R, Farooqui M, Satpute R H & Abed S, *J Drug Deliv Ther*, 8 (2018) 424.
8 Bertinotti F, Giacomello C & Liquori A M, *Acta Cryst*, 9 (1956) 510.
9 Builla J A & Barluenga J, *Het Chem*, 1 (2011) 1.
10 Barton D & Ollis W D, *Comp Org Chem*, (1979) 357.

11 Nandeshwarappa B P, Prakash G K & Sadashiv S O, *Heterocycles-Synthesis and Biological Activities*, (London IntechOpen Limited, UK) 2020.
12 Dlala N A, Bouazizi Y, Ghalla H & Hamdi N, *J Chem*, 2021 (2021) 6674261.
13 Zanina L L, Jimenez D E Q, Jesus M P d, Dinizc L F, Ellena J & Portoa A L M, *J Mol Struc*, 1223 (2020) 129226.
14 H. A. Favre, W. H. Powell. *Nomenclature of Organic Chemistry*, (Royal Society of Chemistry, Cambridge) (2013).
15 Pratap R & Ram V J, *Chem Rev*, 114 (2014) 10476.
16 Tanaka H, Atsumi I, Shirota O, Sekita S, Sakai E, Sato M, Murata J, Murata H, Darnaedi D & Chen I S, *Chem Biodivers*, 8 (2011) 476.
17 Appendino G, Gibbons S, Giana A, Pagani A, Grassi G, Stavri M, Smith E & Rahman M M, *J Nat Prod*, 71 (2008) 1427.
18 Lee Y R & Kim Y M, *Helv Chim Acta*, 90 (2007) 2401.
19 Devakaram R, Black D S, Andrews K T, Fisher G M, Davis R A & Kumar N, *Bioorg Med Chem*, 19 (2011) 5199.
20 Hammam A G, *Ind J Chem*, 44B (2005) 1887.
21 Singh S, Ahmad A, Raghuvanshi D S, Hasanain M, Agarwal K, Dubey V & Khan F, *Bioorg Med Chem Lett*, 26 (2016) 5322.
22 Gourdeau H, Leblond L, Hamelin B, Desputeau C, Dong K, Kianicka I & Drewe J, *Mol Cancer Ther*, 3 (2004) 1375.
23 Parveen M, Malla A M, Yaseen Z, Ali A & Alam M, *J Photochem Photobio B: Biol*, 130 (2014) 179.
24 (a) Ghosh C K, *J Heterocycl Chem*, 20 (1983) 1437; (b) Ghosh C K & Patra A, *J Heterocycl Chem*, 45 (2008) 1529.
25 Desiraju G R, Crystal Engineering: The Design of Organic Solids, (Elsevier, New York) 1989 .
26 Jeffrey G A & Saenger W, *Hydrogen Bonding in Biological Structures*, (Springer, Berlin) 1991.
27 a) Guo F, Yu H, Li L, Xia F, Tong J & Wang B, *Supramol Chem*, 25 (2013) 173.; b) Hazra D K, Ghosh S, Chatterjee P, Ghosh S, Mukherjee M & Mukherjee A K, *Powder Diffr*, 29 (2014) 280.
28 Desiraju G R & Steiner T, *The Weak Hydrogen Bond in Structural Chemistry and Biology*, (Oxford University Press, UK) 1999.
29 Steiner T, *Angew Chem Int Ed*, 41 (2002) 48.
30 Kulaczkowska A D & Mazur L, *J Mol Struc*, 985 (2011) 233.
31 Altomare A, Giacovazzo C, Guagliardi A, Moliterni A G G, Rizzi R & Werner E, *J Appl Cryst*, 33 (2000) 1180.
32 Altomare A, Caliandro R, Camalli M, Cuocci C, Giacovazzo C, Moliterni A G G & Rizzi R, *J Appl Cryst*, 37 (2004) 1025.
33 Le Bail A, Duroy H & Fourquet J L, *Mat Res Bull*, 23 (1988) 447.
34 Toraya H J, *J Appl Cryst*, 19 (1986) 440.
35 Nicolin V F & Cerny R, *J Appl Crystallogr*, 35 (2002) 734.
36 Stewart J J, *J Mol Model*, 13 (2007) 1173.
37 Rietveld H M, *Acta Cryst*, 22 (1967) 151.
38 Larson A C, Von Dreele R B, *Los Alamos National Laboratory Report LAUR* (2000), p. 86.
39 Toby B H, *J Appl Cryst*, 34 (2001) 210.
40 McKinnon J J, Mitchell A S & Spackman M A, *Chem Eur J*, 4 (1998) 2136.
41 Spackman M A & McKinnon J J, *Cryst Eng Comm*, 4 (2002) 378.
42 Wolff S K, Grimwood D J, McKinnon J J, Jayatilaka D, Spackman M A, Crystal Explorer. University of Western Australia, Perth, Australia, 2007. <http://www.ra.bcs.uwa.edu.au/CrystalExplorer/>.
43 Delley B, *Phys Rev*, B66 (2002) 155125.
44 Zhang I Y, Wu J & Xu X, *Chem Comm*, 46 (2010) 3057.
45 (a) David, W I F, Shankland, K, McCusker, L B & Baerlocher C, *Structure Determination from Powder Diffraction Data* (Oxford University Press. Inc., New York) 2002. (b) Harris, K D M, Tremayne, M & Kariuki, B M, *Angew Chem Int Ed*, 40 (2001) 1626.
46 Ishikawa Y, *Acta Cryst*, E70 (2014) 0774.
47 Ishikawa Y, *Acta Cryst*, E71 (2015) 0572.
48 Desiraju G R, Steiner T, *The Weak Hydrogen Bond: In Structural Chemistry and Biology*, (Oxford University Press, Oxford) 1999.
49 Bernstein J, Davis R E, Shimoni L & Chang N L, *Angew Chem Int Ed*, 34 (1995) 1555.
50 Spackman M A & Jayatilaka D, *Cryst Eng Comm*, 11 (2009) 19.
51 McKinnon J J, Spackman M A & Mitchell A S, *Acta Cryst*, B60 (2004) 627.
52 McKinnon J J, Fabbiani F P A & Spackman M A, *Cryst Growth Des*, 7 (2007) 755.
53 Braun D E, Gelbrich T, Kahlenberg V, Laus G, Wieser J & Griesser U J, *New J Chem*, 32 (2008) 1677.
54 Yousuf S, Mukhtar A, Ambreen N, Saad S M & Khan K M, *Acta Cryst*, E68 (2012) 02920.
55 Ishikawa Y, *Acta Cryst*, E70 (2014) 0555.
56 Ishikawa Y, *Acta Cryst*, E70 (2014) 0514.
57 Ishikawa Y, *Acta Cryst*, E70 (2014) 0743.
58 Ishikawa Y, *Acta Cryst*, E70 (2014) 0831.
59 Ishikawa Y, *Acta Cryst*, E70 (2014) 0804.
60 Ishikawa Y, *Acta Cryst*, E70 (2014) 0744.
61 Ishikawa Y, *Acta Cryst*, E70 (2014) 0536.
62 Hazra D K, Mukherjee A K, Helliwellc M & Mukherjee M, *Cryst Eng Comm*, 14 (2012) 993.
63 Hathwar V R, Roopan S M, Subashini R, Khan F N & Row T N G, *J Chem Sci*, 122 (2010) 677.
64 Hazra D K, Mukherjee M, Helliwell M & Mukherjee A K, *Acta Cryst*, C68 (2012) 0452.
65 O'Hagan D, *Chem Soc Rev*, 37 (2008) 308.
66 Wood P A, Olsson T S G, Cole J C, Cottrell S J, Feeder N, Galek P T A, Groom C R & Pidcock E, *Cryst Eng Comm*, 15 (2013) 65.
67 Pallikara I, Skelton J M, Hatcher L E & Pallipurath A R, *Cryst Growth Des*, 24 (2024) 6911.
68 Macrae C F, Sovago I, Cottrell S J, Galek P T A, McCabe P, Pidcock E, Platings M, Shields G P, Stevens J S, Towler M & Wood P A, *J Appl Cryst*, 53 (2020) 226.
69 Kim K H, Han Y K & Jung J, *Theor Chem Acc*, 113 (2005) 233.
70 Aihara J, *J Phys Chem A*, 103 (1999) 7487.